Stochastic finite element method for probabilistic analysis of flow and transport in a three-dimensional heterogeneous porous formation

A. Chaudhuri and M. Sekhar

Department of Civil Engineering, Indian Institute of Science, Bangalore, India

Received 25 November 2004; revised 7 May 2005; accepted 17 May 2005; published 3 September 2005.

[1] A probabilistic study is attempted to analyze the flow and transport in a three-dimensional (3-D) porous formation where the governing parameters are varying randomly in space. It is assumed that the soil parameters, namely, hydraulic conductivity, dispersivity, molecular diffusion, porosity, sorption coefficient, and decay rate, are random fields. A stochastic finite element method (SFEM), which is based on perturbation technique, is developed. The method developed here uses an alternate approach for obtaining improved computational efficiency. The derivatives of the concentration with respect to random parameters are obtained by using the derivatives of local matrices instead of global matrices. This approach increases the computational efficiency of the present method by several orders with respect to standard SFEM. Both accuracy and computational efficiency of this method are compared with that of commonly used Monte Carlo simulation method (MCSM). It is observed that for moderate values of coefficient of variations of the random parameters the mean and standard deviation match reasonably well with MCSM results. Using this method the excessive computational effort required by MCSM can be avoided. In the present study both 1-D as well as 3-D problems are solved to show the advantages of SFEM over MCSM. The correlation scale of the random field is found to be an important parameter. For the range of this parameter studied here it is found that as correlation scale increases, the standard deviation increases. The results obtained for two particular problems in this study show that the coefficient of variation of concentration is higher for the 1-D problem than the 3-D problem.

Citation: Chaudhuri, A., and M. Sekhar (2005), Stochastic finite element method for probabilistic analysis of flow and transport in a three-dimensional heterogeneous porous formation, *Water Resour. Res.*, *41*, W09404, doi:10.1029/2004WR003844.

1. Introduction

[2] Uncertainty in the flow and transport in the groundwater system arises due to the fact that spatial variability of the physical and chemical properties of the system, boundary conditions and source/sink terms are random functions. To quantify the uncertainty, commonly a probabilistic analysis is performed. In the context of flow and transport in porous media such analyses were aimed at assessing the effective medium properties, which are quite different from the laboratory values [*Dagan*, 1989; *Gelhar*, 1993; *Hu et al.*, 1997; *Huang and Hu*, 2000; *Hassan*, 2001; *Chaudhuri and Sekhar*, 2005] as well as on the variability of the head and concentration distributions in terms of their mean and standard deviation [*Tang and Pinder*, 1979; *Dagan*, 1989; *Kapoor and Gelhar*, 1994].

[3] The stochastic partial differential equations (SPDE) for transport, resulting from random properties of the heterogeneous porous medium are either solved using analytical methods [*Dagan*, 1989; *Gelhar*, 1993; *Cushman*, 1997] or numerical methods (Monte Carlo simulations, moment equation method and stochastic finite element method). Analytical methods are not always applicable in real field conditions due to the complicated initial and boundary conditions, source/sink functions, nonuniform flow fields and nonstationary parameters. Under such circumstances, numerical methods are used which often are based on Monte Carlo simulations (MCS). The MCS method is based on generating a large number of equally likely random realizations for obtaining statistical moments of the dependent variable while using a solution of the deterministic system for each realization [*Bellin et al.*, 1992; *Chin and Wang*, 1992; *Osnes*, 1998; *Hassan et al.*, 1999; *Schwarze et al.*, 2001]. This method is computationally exhaustive when a few thousands of realizations are required especially for a higher degree of medium heterogeneities along with higher space-time grid resolution. To avoid the difficulty associated with simulations involving multiple realizations, alternate methods combining perturbation theory with numerical methods (e.g., finite element, finite difference) were developed. One such approach is called stochastic finite element method (SFEM), which has been used in the structural engineering literature [*Kleiber and Hien*, 1992; *Manohar and Ibrahim*, 1999] and for energy distribution modeling [*Osmani*, 2002]. *Spanos and*

0043-1397/05/2004WR003844

Ghanem [1989] used Karhunen-Loeve expansion to represent the random media and an improved Neumann expansion method was employed for static analysis of a beam with random rigidity. An alternate method called projection on homogeneous chaos was proposed by *Ghanem and Spanos* [1991] when the system parameters are varying largely. *Tang and Pinder* [1979] used a perturbation approach with finite difference method for performing uncertainty analysis of solute transport in a one-dimensional porous medium. *Osnes and Langtangen* [1998] presented a probabilistic finite element method for solving stochastic porous media flow problems with a random conductivity field. *Jang et al.* [1994] used reliability method (FORM and SORM) for probabilistic analysis of contaminant transport in 1-D and 2-D heterogeneous porous media. *Zhang* [1999] presented a moment equation method where the dependent variable and the system properties are expressed in terms of an infinite series, which are substituted in the SPDE to solve a flow problem in the vadose zone using a finite difference method. An efficient moment equation method based on Karhunen-Loeve expansions [*Zhang and Lu*, 2004; *Lu and Zhang*, 2004] is proposed for solving flow in stochastic medium. *Zhang* [2002] reviewed various stochastic methods of flow in heterogeneous porous medium.

[4] The objective of the present study is to develop an efficient stochastic finite element method (SFEM) for flow and transport in a general 3-D heterogeneous porous media. The proposed SFEM uses a Laplace transform finite element method, which is found to be efficient for solving the transport equations [*Sudicky and McLaren*, 1992; *Li et al.*, 1992; *Ren and Zhang*, 1999]. In order to improve the computational efficiency of the SFEM by several orders, an approach is proposed wherein the derivatives of the concentration with respect to random parameters are obtained by using the derivatives of local matrices instead of global matrices. The accuracy and the computational efficiency of this method is compared with commonly used Monte Carlo simulation method (MCSM) by applying it on two test problems involving one and three dimensional situations wherein the hydraulic conductivity, dispersivity, molecular diffusion coefficient, porosity, sorption coefficient and first-order decay rate are assumed as random fields. The one dimensional problem uses a time varying boundary condition while the three dimensional problem uses a nonuniform flow field in the domain requiring the use of numerical models. Several cases are analyzed varying the coefficient of variation and correlation scale of the random parameters, while testing the computational efficiency.

2. Formulation

[5] The governing equation for transport of a linearly sorbing and decaying solute in 3-D porous media is

$$(n(\mathbf{x})+\rho_b k_d(\mathbf{x}))\frac{\partial c(\mathbf{x},t)}{\partial t}+\frac{\partial}{\partial x_i}\left(n(\mathbf{x})v_i(\mathbf{x})c(\mathbf{x},t) - n(\mathbf{x})D_{ij}(\mathbf{x})\frac{\partial c(\mathbf{x},t)}{\partial x_j}\right)+\gamma_d(\mathbf{x})c(\mathbf{x},t)=0, \quad (1)$$

where $c(\mathbf{x}, t)$ is the concentration at location $\mathbf{x}$ and time t. Here $n(\mathbf{x})$, $k_d(\mathbf{x})$ and $\gamma_d(\mathbf{x})$ are respectively spatially varying porosity, sorption and decay coefficient. $\mathbf{v}(\mathbf{x})$ is velocity vector which is obtained using hydraulic conductivity tensor ($\mathbf{K}(\mathbf{x})$) and head ($H(\mathbf{x})$), based on,

$$v_i(\mathbf{x})=-K_{ij}(\mathbf{x})\frac{\partial H(\mathbf{x})}{\partial x_j}, \quad (2)$$

It is to be noted that for the equations, the summation over double indices is implied unless otherwise specified. $\mathbf{D}(\mathbf{x})$ is the hydrodynamic dispersion coefficient tensor, which is combined with molecular diffusion coefficient ($D_m(\mathbf{x})$). It is given as

$$D_{ij}\mathbf{x}=\alpha(\mathbf{x})\left((1-\epsilon)\frac{v_i(\mathbf{x})v_j(\mathbf{x})}{v(\mathbf{x})}+\epsilon v(\mathbf{x})\delta_{ij}\right)+D_m(\mathbf{x})\delta_{ij}, \quad (3)$$

where $\alpha(\mathbf{x})$ is the longitudinal local dispersivity and ε is the ratio of transverse to longitudinal local dispersivity. The general initial and boundary conditions are given as

$$c(\mathbf{x},0)=c_0(\mathbf{x}),\ \text{for } \mathbf{x}\in\Omega, c(\mathbf{x},t)=c_b(\mathbf{x},t)\ \text{for } \mathbf{x}\in d\Omega_1$$

and

$$\left(n(\mathbf{x})v_i(\mathbf{x})c(\mathbf{x},t)-n(\mathbf{x})D_{ij}(\mathbf{x})\frac{\partial c(\mathbf{x},t)}{\partial x_j}\right)n_{x_i}=f_b(\mathbf{x},t)\ \text{for } \mathbf{x}\in d\Omega_2 \quad (4)$$

$c_0(\mathbf{x})$ is initial distribution of concentration. $c_b(\mathbf{x}, t)$ and $f_b(\mathbf{x}, t)$ are respectively the time-dependent specified concentration and flux at the boundaries. Here n_{x_i} is the direction cosine of the normal to the boundary surface along x_i axis. The Darcy's equation for steady state flow with spatially varying hydraulic conductivity field is given by

$$\frac{\partial}{\partial x_i}\left(K_{ij}(\mathbf{x})\frac{\partial H(\mathbf{x})}{\partial x_j}\right)=0 \quad (5)$$

and specified boundary conditions governing the flow in the domain,

$$H(\mathbf{x})=H_b(\mathbf{x})\ \text{for } \mathbf{x}\in d\Omega_1.$$

and

$$K_{ij}(\mathbf{x})\frac{\partial H(\mathbf{x})}{\partial x_j}n_{x_i}=q_b(\mathbf{x})\ \text{for } \mathbf{x}\in d\Omega_2. \quad (6)$$

The equation (1) can be solved in the time domain by applying integration or by using the finite difference method. The use of Laplace transform for time is a popular approach to avoid time domain integration. The solution that is obtained in Laplace domain is later transformed to time domain using numerical inverse Laplace transform. In the Laplace space the governing transport equation (1) is given by

$$(s(n(\mathbf{x})+\rho_b k_d(\mathbf{x}))+\gamma_d(\mathbf{x}))\hat{c}(\mathbf{x},s) + \frac{\partial}{\partial x_i}\left(n(\mathbf{x})v_i(\mathbf{x})\hat{c}(\mathbf{x},s)-n(\mathbf{x})D_{ij}(\mathbf{x})\frac{\partial\hat{c}(\mathbf{x},s)}{\partial x_j}\right)=c_0(\mathbf{x}), \quad (7)$$

where s is the Laplace parameter. In the present study equation (7) is solved using FEM after applying Laplace transform to the boundary conditions. Prior to solving

equation (7) with FEM the velocity field is obtained by solving equation (5).

3. Deterministic FEM Formulation

[6] In FEM the concentration inside an element is expressed as $\widehat{c}(\mathbf{x}, s) = \sum_{k=1}^{n} N_k(\mathbf{x})\widehat{C}_k(s)$, where n is the number of nodes per element. $N_k(\mathbf{x})$ and $\widehat{C}_k(s)$ are respectively kth shape function and concentration at kth node. For pth element the equation is obtained as

$$\begin{aligned}\int_{\Omega^e}\Bigg[&\Big(s\big(n_p+\rho_b k_{d_p}\big)+\gamma_{d_p}\Big)N_k(\mathbf{x})N_l(\mathbf{x})\\&-\frac{\partial N_k(\mathbf{x})}{\partial x_i}\left(n_p v_{ip}N_l(\mathbf{x})-n_p D_{ij_p}\frac{\partial N_l(\mathbf{x})}{\partial x_j}\right)\Bigg]d\mathbf{x}\widehat{C}_l(s)\\&+\oint_{d\Omega^e}N_k(\mathbf{x})\left(n_p v_{i_p}N_l(\mathbf{x})-n_p D_{ij_p}\frac{\partial N_l(\mathbf{x})}{\partial x_j}\right)n_{x_i}dS\widehat{C}_l(s)\\&=\int_{\Omega_e}N_k(\mathbf{x})c_0(\mathbf{x})d\mathbf{x},\end{aligned}\tag{8}$$

$$\Rightarrow [D(s)]_p\left\{\widehat{C}(s)\right\}_p=\{C_0(s)\}_p\tag{9}$$

Here the suffix 'p' corresponds to the property of pth element. The domain is discretized with N elements. The global equations for the transport and flow are obtained as

$$[D(s)]\left\{\widehat{C}(s)\right\}=\{C_0(s)\}\text{ and }[K]\{H\}=\{H_0\}.\tag{10}$$

The global dynamic transport matrix $[D(s)]$ and source vector $\{C_0(s)\}$ are obtained using the given initial and boundary conditions. Numerical inverse Laplace transform [*Brancik*, 2000] is applied on the solution of equation (10). For flow $[K]$ is the global hydraulic conductivity matrix. The ith component of velocity of pth element is obtained by taking average of velocity at all Gauss points ($\mathbf{x}_k$, for $k = 1, \ldots, N_G$, where N_G is the number of Gauss points), and it is given as

$$v_{i_p}=-\frac{1}{N_G}K_{ij_p}\sum_{k=1}^{N_G}\left.\frac{\partial N_l(\mathbf{x})}{\partial x_j}\right|_{\mathbf{x}_k}H_l=-\frac{1}{N_G}K_p\sum_{k=1}^{N_G}\left.\frac{\partial N_l(\mathbf{x})}{\partial x_i}\right|_{\mathbf{x}_k}H_l.\tag{11}$$

Here l implies summation over repeated indices. For isotropic cases the hydraulic conductivity tensor becomes a scalar quantity (K_p).

4. SFEM Formulation

[7] For a perturbation method, the properties which are varying randomly in space are decomposed into a mean component and a zero mean random component. In a perturbation based SFEM, for each element, the properties which are treated as random variables are also decomposed as $K_p = \overline{K}_p + K'_p$, $\alpha_p = \overline{\alpha}_p + \alpha'_p$, $n_p = \overline{n}_p + n'_p$, $k_{d_p} = \overline{k}_{d_p} + k'_{d_p}$, $\gamma_{d_p} = \overline{\gamma}_{d_p} + \gamma'_{d_p}$ and $D_{m_p} = \overline{D}_{m_p} + D'_{m_p}$. The velocity and dispersion coefficient can also be written as $v_{i_p} = \overline{v}_{i_p} + v'_{i_p}$ and $D_{ij_p} = \overline{D}_{ij_p} + D'_{ij_p}$ respectively. For statistically homogeneous random field, the mean of the properties for each element remain same. Hence the matrices $[K]$ and $[D(s)]$ are also decomposed into mean ($[\overline{K}]$ and $[\overline{D}(s)]$) and zero mean fluctuating components ($[K]'$ and $[D(s)]'$). The zero mean random component of dynamic transport matrix $[D(s)]'$ is a linear function of random variables r'_p. Here r'_p, ($p = 1, 2, \ldots, N_r$) are the velocity components, local dispersivity, molecular diffusion, porosity, sorption coefficient and decay rate of each element. N_r is the total number of random variables and in this study $N_r = 8N_e$, where N_e is the total number of elements. Expanding $[D(s)]$ using Taylor series and noting that 2nd and higher-order derivatives vanish being a linear case,

$$[D(s)]=\left[\overline{D}(s)\right]+[D(s)]'=\left[\overline{D}(s)\right]+\sum_{p=1}^{N_r}[D(s)]^I_{r_p}r'_p\tag{12}$$

where $[D(s)]^I_{r_p}=\frac{\partial[D(s)]}{\partial r_p}$. Thus the FE equation for transport equation (10) is written as

$$\left(\left[\overline{D}(s)\right]+\sum_{p=1}^{N_r}\left[D(s)]^I_{r_p}r'_p\right]\right)\left\{\widehat{C}(s)\right\}=\{C_0(s)\}.\tag{13}$$

The concentration is obtained from equation (13) and after decomposition it is written as

$$\begin{aligned}\left\{\widehat{\overline{C}}(s)\right\}+\left\{\widehat{C}(s)\right\}'&=\left(\left[\overline{D}(s)\right]+\sum_{p=1}^{N_r}[D(s)]^I_{r_p}r'_p\right]\right)^{-1}\{C_0(s)\}\\&=\Bigg([I]-\sum_{p=1}^{N_r}\left[\overline{D}(s)\right]^{-1}[D(s)]^I_{r_p}r'_p+\sum_{p=1}^{N_r}\sum_{q=1}^{N_r}\left[\overline{D}(s)\right]^{-1}\\&\quad\cdot[D(s)]^I_{r_p}\left[\overline{D}(s)\right]^{-1}[D(s)]^I_{r_q}r'_pr'_q+\cdots\Bigg)\left[\overline{D}(s)\right]^{-1}\{C_0(s)\}.\end{aligned}\tag{14}$$

It may be noted that the local dynamic transport matrix ($[D(s)]_q$) of qth element is only a function of random variables (n_q, k_{dq}, γ_{d_q}, v_{1q}, v_{2q}, v_{3q}, α_q and d_{mq}). Hence the derivative $[D(s)]^I_{q,r_p}$ only exists if the random variable r_p corresponds to any one of the above mentioned random variables and $[D(s)]^I_{q,r_p}$ vanishes when r_p corresponds to any property of an element except qth element. Hence the derivative of the global matrix, $[D(s)]^I_{r_p}$, has nonzero entry in the position corresponding to qth element when r_p is a parameter of qth element. In this case the collection of all nonzero entries in $[D(s)]^I_{r_p}$ forms a matrix of the size same as $[D(s)]_q$. Using nodal connectivity matrix, the matrix multiplication of $[\overline{D}(s)]^{-1}[D(s)]^I_{rp}$ in equation (14) can be reduced to $((N \times n) \times (n \times n))$ from $((N \times N) \times (N \times N))$, where N and n are respectively total number of nodes in domain and number of nodes per element. Thus by following this approach the computational efficiency increases by the order of (N^2/n^2). For example using the present approach in a 3-D problem with a brick element ($n = 8$) and a total number of nodes $N = 800$, the above factor results in a computational efficiency of 10^4, if simplistic matrix multiplication algorithm is used. This efficiency factor still remains quite significant (at least two orders) even if better matrix multiplication algorithms (such as used in commercial packages BLAS, LAPACK) are employed. After taking the expectation for the equation (14), the mean concentration ($\{\widehat{\overline{C}}(s)\}$)is obtained as

$$\begin{aligned}\left\{\widehat{\overline{C}}(s)\right\}=\Bigg([I]+\sum_{p=1}^{N_r}\sum_{q=1}^{N_r}\left[\overline{D}(s)\right]^{-1}[D(s)]^I_{r_p}\left[\overline{D}(s)\right]^{-1}[D(s)]^I_{r_q}\overline{r'_pr'_q}+\cdots\Bigg)\\\cdot\left[\overline{D}(s)\right]^{-1}\{C_0(s)\}.\end{aligned}\tag{15}$$

In the above expression the mean is second-order accurate. The equation for the perturbed component ($\{\widehat{C}'(s)\}$) is obtained by subtracting equation (15) from equation (14). When $r'_p r'_q - \overline{r'_p r'_q}$ is neglected, the equation reduces to,

$$\begin{aligned}\left\{\widehat{C}(s)\right\}' &= \sum_{p=1}^{N_r}\left\{\widehat{C}(s)\right\}^I_{r_p} r'_p,\\ \left\{\widehat{C}(s)\right\}^I_{r_p} &= -\left[\overline{D}(s)\right]^{-1}[D(s)]^I_{r_p} r'_p \left[\overline{D}(s)\right]^{-1}\{C_0(s)\}.\end{aligned} \tag{16}$$

Using numerical inverse Laplace transform, the mean concentration ($\{\overline{C}(t)\}$) and the random component of concentration ($\{C'(t)\}$) in time domain are obtained. The covariance matrix is obtained after applying numerical inverse Laplace transform to equation (16), which is expressed as

$$\begin{aligned}\overline{\{C(t_1)\}'\{C(t_2)\}'^T} &= \sum_{p=1}^{N_r}\sum_{q=1}^{N_r}\mathcal{L}^{-1}\left[\left\{\widehat{C}(s_1)\right\}^I_{r_p}\right]\mathcal{L}^{-1}\left[\left\{\widehat{C}(s_2)\right\}^I_{r_q}\right]^T \overline{r'_p r'_q}\\ &= \mathcal{L}^{-1}\left[\mathcal{L}^{-1}\left[\sum_{p=1}^{N_r}\sum_{q=1}^{N_r}\left\{\widehat{C}(s_1)\right\}^I_{r_p}\left\{\widehat{C}(s_2)\right\}^{I^T}_{r_q}\overline{r'_p r'_q}\right]\right].\end{aligned} \tag{17}$$

The computational time required depends on the discretization in the Laplace space and the number of finite elements. When the number of elements used for discretization is small, the last expression in equation (17) is computationally faster. Similarly perturbation approach can be applied on flow equation, to obtain the mean and perturbed component of hydraulic head. For flow the random properties are only the hydraulic conductivity of the elements (K_p, p = 1, 2, …, N_k), here $N_k = N_e$. Therefore the mean and perturbed component of hydraulic head are expressed as

$$\begin{aligned}\{\overline{H}\} = &\left([I] + \sum_{p=1}^{N_k}\sum_{q=1}^{N_k}\left[\overline{K}\right]^{-1}[K]^I_{K_p}\left[\overline{K}\right]^{-1}[K]^I_{K_q}\overline{K'_p K'_q} + \cdots\right)\\ &\cdot\left[\overline{K}\right]^{-1}\{H_0\};\end{aligned} \tag{18}$$

$$\begin{aligned}\{H\}' &= \sum_{p=1}^{N_k}\{H\}^I_{K_p}K'_p,\\ \{H\}^I_{K_p} &= -\left[\overline{K}\right]^{-1}[K]^I_{K_p}\left[\overline{K}\right]^{-1}\{H_0\}.\end{aligned} \tag{19}$$

Using equations (18) and (19) the mean and random component of v_{ip} are obtained as

$$\overline{v}_{ip} = -\frac{1}{N_G}\sum_{k=1}^{N_G}\left.\frac{\partial N_l(\mathbf{x})}{\partial x_i}\right|_{\mathbf{x}_k}\left(\overline{K}_p\overline{H}_l + \sum_{q=1}^{N_k}H^I_{l,K_q}\overline{K'_p K'_q}\right) \tag{20}$$

$$v'_{ip} = -\sum_{q=1}^{N_k}\frac{1}{N_G}\sum_{k=1}^{N_G}\left.\frac{\partial N_l(\mathbf{x})}{\partial x_i}\right|_{\mathbf{x}_k}\left(\overline{H}_l\delta_{pq} + \overline{K}_p H^I_{l,K_q}\right)K'_q = \sum_{q=1}^{N_k}v^I_{ip,K_q}K'_q \tag{21}$$

Here l implies summation over repeated indices. From the expression of perturbed component of velocity one can obtain the auto covariance of velocity and cross covariance with any other random properties (r'_j) using the auto covariance of hydraulic conductivity and cross covariance of hydraulic conductivity with r'_j, which is expressed as

$$\overline{v'_{i_{p_1}}v'_{j_{p_2}}} = \sum_{q_1=1}^{N_k}\sum_{q_2=1}^{N_k}v^I_{i_{p_1},K_{q_1}}v^I_{j_{p_2},K_{q_2}}\overline{K'_{q_1}K'_{q_2}} \text{ and } \overline{v'_{ip}r'_j} = \sum_{q=1}^{N_k}v^I_{ip,K_q}\overline{K'_q r'_j}. \tag{22}$$

Here the mean velocity is second-order accurate while the covariance of velocity is first-order accurate as the term ($K'_p K'_q - \overline{K'_p K'_q}$) is neglected. The mean of the resultant velocity and its random component are expressed as

$$\overline{v}_p = v_p + \frac{1}{v_p}\sum_{i=1}^{3}C_{v_{ip}v_{ip}} - \frac{1}{v_p^3}\sum_{i=1}^{3}\sum_{j=1}^{3}\overline{v}_{i_p}\overline{v}_{j_p}C_{v_{i_p}v_{j_p}} \text{ and } v'_p = \frac{1}{v_p}\sum_{i=1}^{3}\overline{v}_{i_p}v'_{i_p}. \tag{23}$$

Here $v_p = \left[\sum_{i=1}^{3}\overline{v}_{ip}^2\right]^{1/2}$. The effective mean hydrodynamic dispersion coefficient and its random component are obtained by using equation (3), which are given as

$$\begin{aligned}\overline{D}_{ij_p} = &\left(\overline{\alpha}_{Lp}\left(\frac{\overline{v}_{ip}\overline{v}_{jp} + C_{v_{ip}v_{jp}}}{\overline{v}} - \frac{\overline{v}_{ip}C_{v_{jp}v_p} + \overline{v}_{jp}C_{v_{ip}v_p}}{\overline{v}_p^2} + \frac{\overline{v}_{ip}\overline{v}_{jp}C_{v_pv_p}}{\overline{v}_p^3}\right)\right.\\ &\left. + \frac{\overline{v}_{ip}C_{v_{jp}\alpha_{Lp}} + \overline{v}_{jp}C_{v_{ip}\alpha_{Lp}}}{\overline{v}_p} - \frac{\overline{v}_{ip}\overline{v}_{jp}C_{v_p\alpha_{Lp}}}{\overline{v}_p^2}\right)\\ &\cdot(1-\epsilon) + \epsilon\left(\overline{\alpha}_{Lp}\overline{v}_p + C_{v_p\alpha_{Lp}}\right)\delta_{ij} + \overline{D_{mp}}\delta_{ij}\end{aligned} \tag{24}$$

$$\begin{aligned}D'_{ij_p} = &\left(\overline{\alpha}_{Lp}\left(\frac{\overline{v}_{ip}v'_{jp} + \overline{v}_{jp}v'_{ip}}{\overline{v}_p} - \frac{\overline{v}_{ip}\overline{v}_{jp}v'_p}{\overline{v}_p^2}\right) + \alpha'_{Lp}\frac{\overline{v}_{ip}\overline{v}_{jp}}{\overline{v}_p}\right)(1-\epsilon)\\ &+ \epsilon\left(\overline{\alpha}_{Lp}v'_p + \alpha'_{Lp}\overline{v}_p\right)\delta_{ij} + D'_{mp}\delta_{ij}.\end{aligned} \tag{25}$$

To obtain the expression of D'_{ij_p}, the difference between the product of two perturbed components and the mean of that product, is neglected.

5. Description of the Random Fields

[8] The hydraulic conductivity which varies randomly in space, is commonly modeled as a random field with a log normal distribution since it takes positive values and varies in several orders [*Gelhar*, 1993; *Cushman*, 1997]. *Hassan* [2001] assumed that the porosity follows a log normal distribution and studied the effect of its correlation with hydraulic conductivity. The sorption coefficient on the other hand has been modeled either as normal or log normal distribution in the literature [*Wu et al.*, 2004; *Hu et al.*, 1997]. Similarly decay rate can be considered to follow either normal or log normal distribution [*Miralles-Wilhelm and Gelhar*, 2000; *Metzger et al.*, 1999]. Commonly, the distribution of dispersion coefficient can be derived from the input distribution of local dispersivity, hydraulic conductivity and diffusion coefficient. *Harleman et al.* [1963] gave an empirical relationship between dispersivity and

hydraulic conductivity. This relationship results in a log normal distribution for dispersivity when hydraulic conductivity is assumed to follow log normal distribution. *Haggerty and Gorelick* [1995], suggested the use of either a uniform or log normal distribution for diffusion coefficient. On the basis of the above studies and absence of specific experimental data pertaining to the choice of distributions, in this study the flow and transport parameters, which are considered as random fields, are assumed to follow a log normal distribution since they take positive values and also vary considerably. Hence the hydraulic conductivity, dispersion coefficient, porosity, sorption coefficient and decay can be expressed as $K(\mathbf{x}) = K_G \exp(f_K(\mathbf{x}))$, $D(\mathbf{x}) = D_G \exp(f_D(\mathbf{x}))$, $n(\mathbf{x}) = n_G \exp(f_n(\mathbf{x}))$ $k_d(\mathbf{x}) = k_{d_G} \exp(f_{k_d}(\mathbf{x}))$, $\gamma_d(\mathbf{x}) = \gamma_{d_G} \exp(f_\gamma(\mathbf{x}))$ and $D_m(\mathbf{x}) = D_{m_G} \exp(f_{D_m}(\mathbf{x}))$. The standard deviation of log hydraulic conductivity and the geometric mean of hydraulic conductivity are obtained as $\sigma_{f_K} = \sqrt{\log\left(1 + \frac{\sigma_K^2}{\overline{K}^2}\right)}$ and $K_G = \overline{K} - \frac{\sigma_{f_K}^2}{2}$. The random fields are assumed as statistically homogeneous and described by a Gaussian (squared exponential) type correlation function. However, it may be noted that for specific applications experimentally derived correlations functions can be applied in the SFEM. The correlation coefficient between the properties of any two points is given as $\rho(\mathbf{x}) = (-(\frac{x_1}{\lambda_1})^2 - (\frac{x_2}{\lambda_2})^2 - (\frac{x_3}{\lambda_3})^2)$. The covariance matrix for random element properties is determined from the correlation function using the local averaging method. For this correlation function the closed form expression of correlation coefficient of random properties of any two elements as given by *Vanmarcke* [1983] is

$$\rho_{f_p f_q} = \frac{1}{V_p V_q}\int_{V_p}\int_{V_q}\rho(\mathbf{x}_p - \mathbf{x}_q)d\mathbf{x}_p d\mathbf{x}_q = \frac{1}{8V_pV_q}\sum_{i=0}^{3}\sum_{j=0}^{3}\sum_{k=0}^{3}(-1)^{(i+j+k)}(L_{1i}L_{2j}L_{3k})^2\gamma(L_{1i},L_{2j},L_{3k}), \tag{26}$$

where

$$\gamma(L_{1i},L_{2j},L_{3k}) = \frac{8}{L_{1i}L_{2j}L_{3k}}\int_0^{L_{3k}}\int_0^{L_{2j}}\int_0^{L_{1i}}\left(1-\frac{x_1}{L_{1i}}\right)\left(1-\frac{x_2}{L_{2j}}\right)\cdot\left(1-\frac{x_3}{L_{3k}}\right)\times\rho(x_1,x_2,x_3)dx_1dx_2dx_3 = \gamma_{1D}(L_{1i})\gamma_{1D}(L_{2j})\gamma_{1D}(L_{3k}), \tag{27}$$

and $\gamma_{1D}(L_{ij}) = (\frac{\lambda_i}{L_{ij}})^2\,[\sqrt{\pi}\frac{L_{ij}}{\lambda_i}\,\mathrm{erf}\,(\frac{L_{ij}}{\lambda_i}) + \exp\,(\frac{L_{ij}}{\lambda_i}) - 1]$. The various intervals are shown in Figure 1. The correlation coefficient between K_i and k_{dj} is determined as

$$\rho_{K_i k_{dj}} = \frac{K_G k_{dG}}{\sigma_K \sigma_{k_d}}\exp\left(\frac{1}{2}\left(\sigma_{f_K}^2 + \sigma_{f_{k_d}}^2\right)\right)\left(\exp\left(\rho_{f_{K_i}f_{k_{dj}}}\sigma_{f_K}\sigma_{f_{k_d}}\right) - 1\right). \tag{28}$$

In a similar fashion the correlation between any other two random parameters can be obtained.

6. Results and Discussions

[9] The stochastic finite element method (SFEM) developed above is applied to study the migration of contaminant from a waste dump. Both 1-D and 3-D problems are used for modeling the system. The accuracy of SFEM is verified by comparing with MCSM for both these problems. The testing with both of these problems is made to assess the accuracy and computational efficiency of the SFEM affected by the dimension of the problem and to demonstrate the use of relatively complicated time varying boundary conditions. In both of these problems the studies are carried out to show the effect of coefficient of variation (COV) of the random parameters.

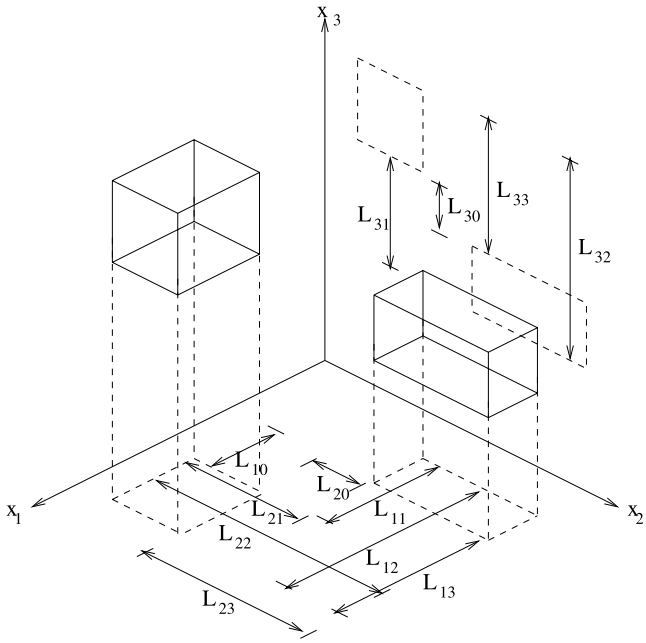

Figure 1. Definition of various distances characterizing the relative position of two elements.

6.1. One-Dimensional Problem

[10] A 1-D model may be acceptable [*Rowe and Booker*, 1986] for analyzing the transport of pollutant in the soil liner underlying a landfill, when the velocity of flow is essentially vertical and uniform. For describing the system conveniently, the parameters and the variables are made dimensionless with respect to thickness of the soil liner (h) and vertical velocity of flow for the deterministic problem (v_d). In this problem the time varying boundary conditions for concentration [*Rowe and Booker*, 1986] are used, which are given as

$$c(x_3,t) = 1 + \frac{1}{h_f}\int_0^t n(x_3)\left(v(x_3)c(x_3,\tau) - D(x_3)\frac{\partial c(x_3,\tau)}{\partial x_3}\right)d\tau \quad \text{at } x_3 = 0,$$
$$c(x_3,t) = \frac{1}{n_b h_b}\int_0^t n(x_3)\left(v(x_3)c(x_3,\tau) - D(x_3)\frac{\partial c(x_3,\tau)}{\partial x_3}\right)d\tau - \frac{v_b}{n_b L}\int_0^t c(x_3,\tau)d\tau \quad \text{at } x_3 = 1. \tag{29}$$

Here $c(x_3, t) = \tilde{c}(\tilde{x}_3, \tilde{t})/c_0$ is the dimensionless concentration of the pollutant at dimensionless depth ($x_3 = \tilde{x}_3/h$) and dimensionless time ($t = v_d\,\tilde{t}/h$). Further, $v(x_3) = \tilde{v}(\tilde{x}_3)/v_d$, $D(x_3) = \widetilde{D}(\tilde{x}_3)/(v_d h)$ and $\gamma_d(x_3) = \tilde{\gamma}_d(\tilde{x}_3)h/v_d$ are respectively

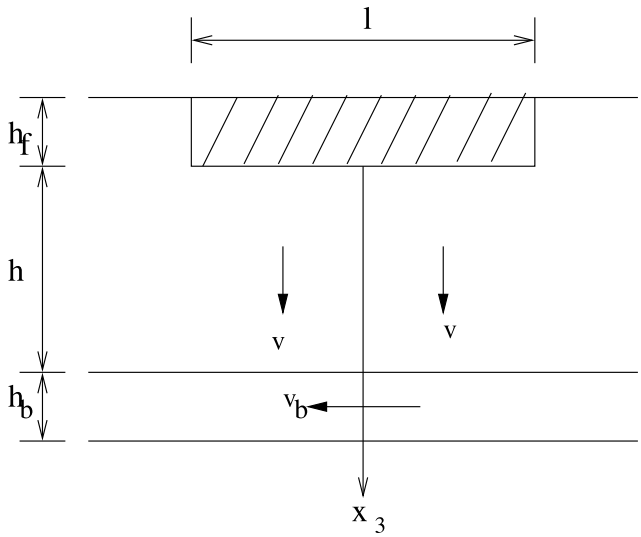

Figure 2. A schematic diagram of vertical leachate transport to the soil from a landfill for the 1-D test case.

the dimensionless vertical velocity of flow in the soil liner, the dispersion coefficient, the decay coefficient. The equivalent dimensionless height of the landfill is given by $h_f = \tilde{h}_f/h$. In addition $h_b = \tilde{h}_b/h$, $v_b = \tilde{v}_b/v_d$ and n_b are respectively the height of the permeable layer (or sandy aquifer), the horizontal velocity of flow and porosity of the sandy aquifer and $L = \tilde{L}/h$ is the dimensionless length of the landfill as shown in Figure 2. Here$\tilde{}$ corresponds to the dimensional quantity. Hydraulic conductivity, porosity, dispersion coefficient and sorption coefficient are assumed to vary randomly along the vertical direction. In the present study, it is assumed that all of the random governing parameters have the same covariance function. The problem is solved using the following values of the parameters, $\overline{k}_d = 1.0$, $\gamma_d = 2.0$, $v_b = 1000$, $h_f = 1.0$, $\overline{D} = 1.0$, $\overline{n} = 0.45$, $h_b = 1.0$, $n_b = 0.3$ and $L = 40$. The comparison between SFEM and MCSM (with 10000 realizations) is made in terms of mean, standard deviation and computational time as presented in Table 1. The results are provided for various coefficient of variations. The concentration is measured at the bottom of the soil liner. The mean and standard deviation of the concentration are shown in Figure 3. The accuracy of SFEM is compared with MCSM for a range of coefficient of variation of random parameters and correlation scales (λ),

Table 1. Values of Statistical Parameters and Comparison of Results for Different Cases in the 1-D Problem[a]

	COV					Error, %			
Case	n	k_d	K	d_m	λ	$\overline{c}_p$	$t_{\overline{c}_p}$	σ_{c_p}	$t_{\sigma_{cp}}$
1A1	0.025	0.02	0.05	0.02	0.5	−0.01	0.00	−0.20	0.24
1A2	0.100	0.10	0.25	0.10	0.5	−0.10	−0.16	1.50	3.50
1A3	0.250	0.20	0.50	0.20	0.5	−0.68	−1.40	7.50	15.80
1B1	0.025	0.02	0.05	0.02	1.0	0.02	0.00	−0.27	0.24
1B2	0.100	0.10	0.25	0.10	1.0	0.06	−0.16	0.37	5.90
1B3	0.250	0.20	0.50	0.20	1.0	0.12	−4.10	3.00	27.80
1C1	0.025	0.02	0.05	0.02	2.0	−0.01	0.00	0.02	0.24
1C2	0.100	0.10	0.25	0.10	2.0	−0.01	−0.16	0.05	6.70
1C3	0.250	0.20	0.50	0.20	2.0	1.11	−6.00	0.50	35.10

[a]CPU time is 0.02 s for SFEM and 37 s for MCSM.

and the results are presented in Table 1. The mean concentration behavior obtained from SFEM matches well with that of MCSM (a maximum of 1.1% for all the cases studied here). Coefficient of variation of random parameters affects the arrival time (t_{c_p}) of peak of mean concentration ($\overline{c}_p$). The SFEM estimates early arrival of the peak in comparison to MCSM by a maximum of 6% for the cases. The comparison between SFEM and MCSM for the standard deviation of concentration (σ_{c_p}) indicates that the results of SFEM are found to be less than 7.5% for various cases studied. As expected higher errors are noted for higher coefficient of variation. The SFEM is found to overestimate the peak value of the standard deviation of concentration (σ_{c_p}) and results in a later arrival ($t_{\sigma_{cp}}$) of this peak. The magnitude of the error in the arrival of peak values of the mean and standard deviation of concentrations increases with increase in correlation scale. The computations for all the test cases of this problem are performed on COMPAQ Alpha Server ES40 (a cluster of four CPUs with 667 MHz).

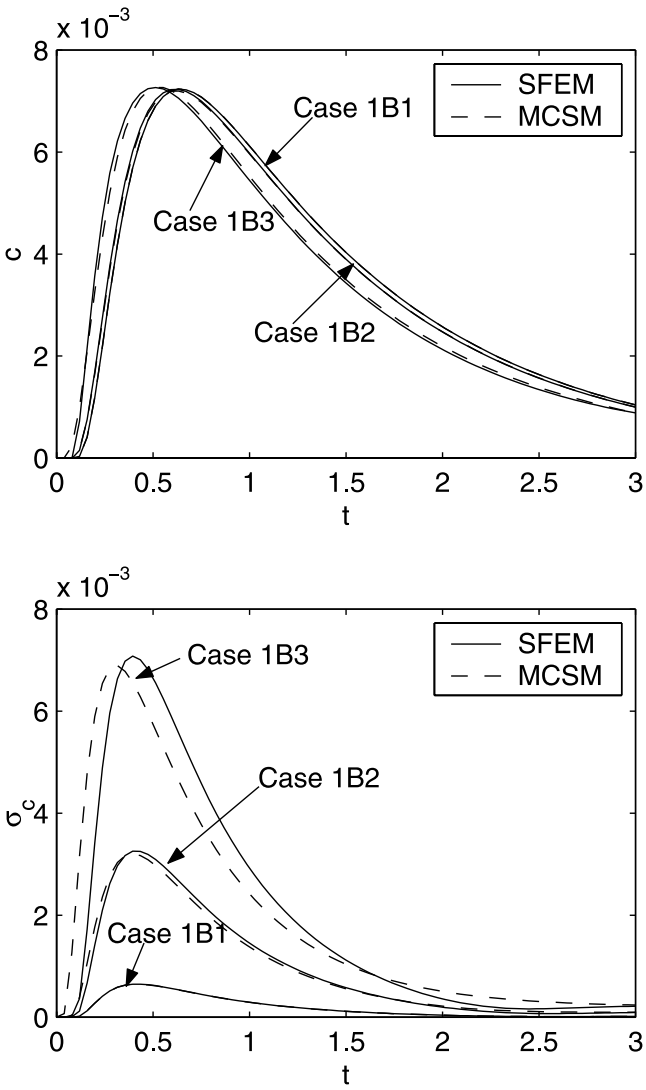

Figure 3. Comparison of results obtained by SFEM and MCSM, for the 1-D test problem (a) Mean and (b) standard deviation of concentration at the bottom of the soil liner for $\lambda = 1.0$.

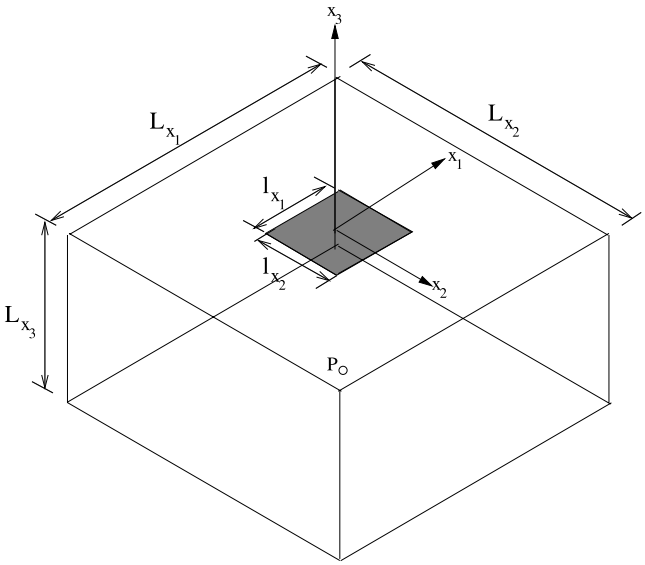

Figure 4. A schematic diagram of 3-D problem with a continuous source at the top.

It is found that the computational time taken by SFEM is approximately equal to 5 to 6 times that of the solution of the deterministic FEM.

6.2. Three-Dimensional Problem

[11] The SFEM developed in section 4 is applied to study the probabilistic behavior of concentration distribution in the 3-D aquifer/permeable layer (Figure 4). The porosity, decay coefficient, sorption coefficient, hydraulic conductivity, dispersivity and molecular diffusion are considered as spatially varying random fields. In this study the correlation scales along the horizontal plane is assumed to be same (i.e., $\lambda_1 = \lambda_2 = \lambda_h$). The horizontal correlation scale (λ_h) is considered much larger in comparison to the vertical correlation scale (λ_3). Here λ_3 is taken as one tenth of λ_h. The flow field in this problem becomes nonuniform due to the constant continuous recharge from the pollutant source combined with lateral groundwater flow in the permeable layer.

[12] The mean and covariance of the random flow field is derived from the random hydraulic conductivity field. Along with covariance matrices of the other random fields, the covariance of velocity is also used for the probabilistic analysis of contaminant transport. A square contaminant source of dimension $l_{x_1} = l_{x_2} = l$ is assumed to be located in an aquifer. The governing equation (1), the boundary conditions in Section 2 and the parameters are made dimensionless with respect to the size of the source and the horizontal velocity of flow. Here $c(\mathbf{x}, t) = \tilde{c}(\tilde{\mathbf{x}}, \tilde{t})/c_0$ is the dimensionless concentration of the pollutant at a dimensionless distance $\mathbf{x} = \tilde{\mathbf{x}}/l$, a dimensionless time ($t = v_d\tilde{t}/l$) and c_0 is the concentration at the top of the soil. Further, $v(\mathbf{x}) = \tilde{v}(\tilde{\mathbf{x}})/v_d$, $\alpha(\mathbf{x}) = \tilde{\alpha}(\tilde{\mathbf{x}})/l$, $D_m(\mathbf{x}) = \tilde{D}_m(\tilde{\mathbf{x}})/(v_d l)$, $\gamma_d(\mathbf{x}) = \tilde{\gamma}_d(\tilde{\mathbf{x}})l/v_d$ and $q = \tilde{q}/v_d$ are respectively the dimensionless velocity of flow, dispersivity, molecular diffusion, decay coefficient and recharge at the top. Here v_d is the horizontal velocity of flow, for a deterministic case without any recharge. The following numerical values of parameters are chosen for solving the 3-D problem: $\overline{n} = 0.4$, $\overline{k}_d = 0.5$, $\overline{\gamma}_d = 1.0$, $\overline{\alpha} = 0.5$, $\overline{D}_m = 1.0$ and $q = 0.01$.

[13] The comparison between SFEM and MCSM (with 10000 realizations) for different sets of coefficient of variation and correlation scale of random parameters, is made in terms of mean and standard deviation, which are presented in Figures 5 and 6. The test cases comprise two correlation scales $\lambda_h = 2$ and $\lambda_h = 4$ and a range of coefficient of variations. Higher correlation scales are avoided because of the smaller computational domain of this problem used as well as due to relatively lesser sensitivity of the results at higher value of correlation length as demonstrated by *Zhang and Lu* [2004]. The maximum coefficient of variation used is 125% for hydraulic conduc-

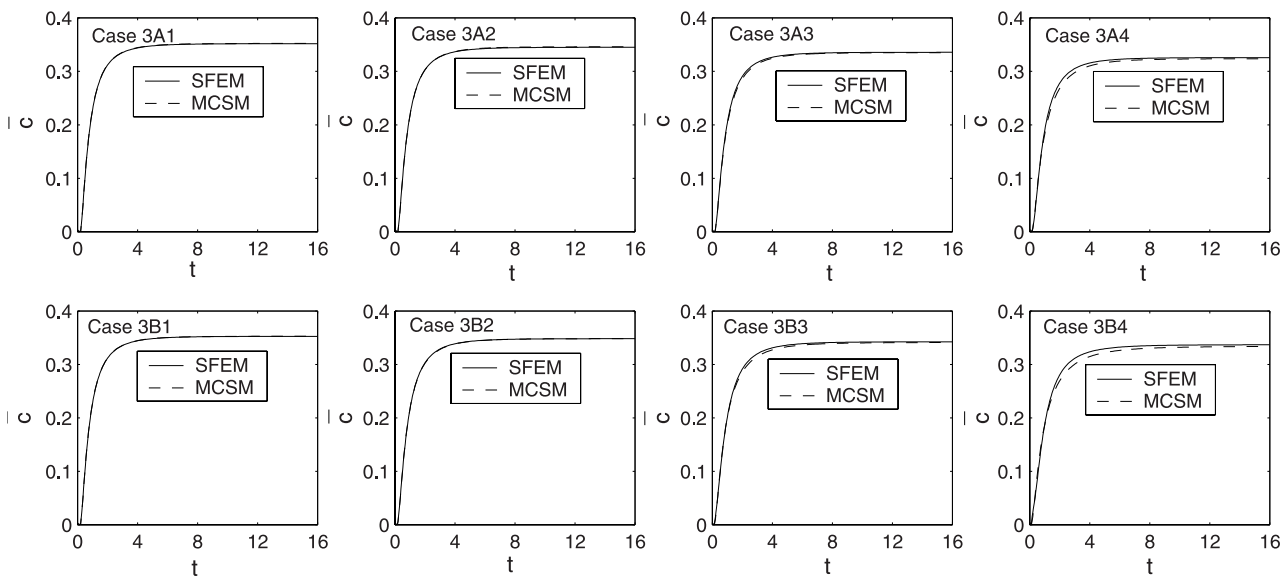

Figure 5. Comparison of results obtained by SFEM and MCSM for the 3-D test problem, (top) mean and (bottom) standard deviation of concentration at the bottom of the soil liner for different cases.

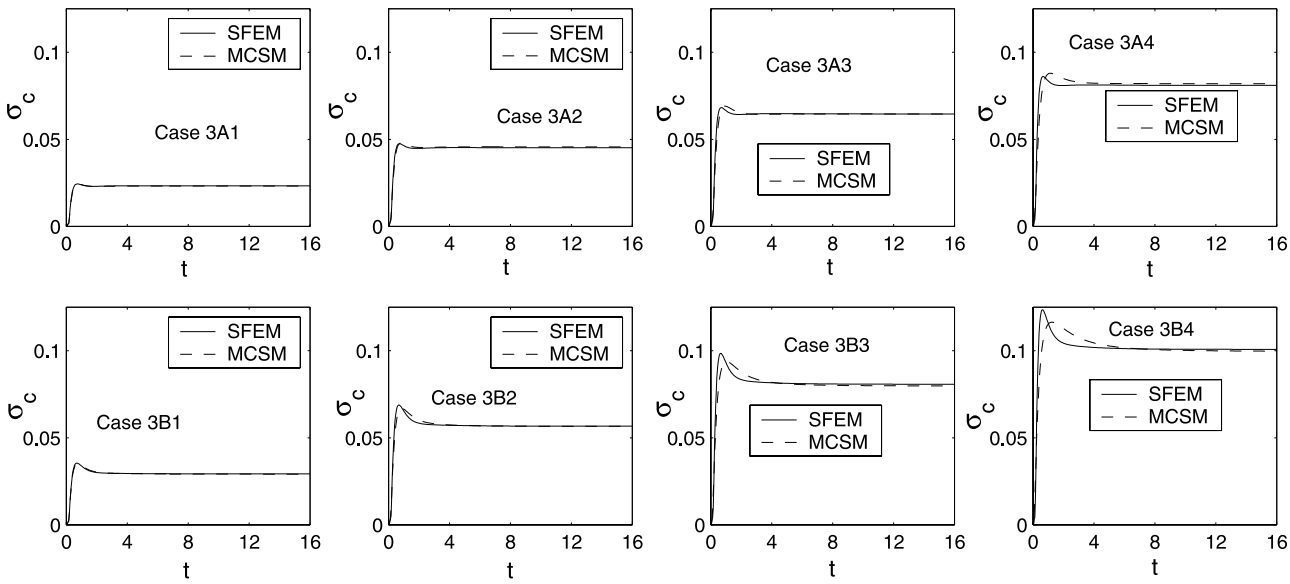

Figure 6. Comparison of results obtained by SFEM and MCSM for the 3-D test problem, (top) mean and (bottom) standard deviation of concentration at the bottom of the soil liner for different cases.

tivity and 50% for rest of the other random parameters. Since the perturbation based method used here is first-order accurate for standard deviation and second-order accurate for the mean, it is expected that the results at higher variances (greater than 1.0) may result in higher errors. Figures 5 and 6 show the $\overline{c}$ and σ_c respectively for various test cases (as listed in Table 2) obtained using both SFEM and MCSM. These results are obtained in terms of evolution of steady state concentration at the bottom of the permeable layer at exactly below the center of the source (at point P shown in Figure 4). Since at this location relatively higher concentrations would result at the top of the impermeable layer, the comparison between the two methods is made at this location. The mean concentration ($\overline{c}$) is found to increase exponentially and shows an asymptotic behavior while the σ_c of concentration shows a peak followed by a lower steady state value. The finite value of standard deviation of concentration at asymptotic time is due to the presence of decay parameter and this finite value depends on the decay coefficient and the distance from the source. The shift in time of the peak values of σ_c between SFEM and MCSM in the Figure 6 for higher correlation scale and variance could be due to use of incorrect effective velocity and covariance of random velocity field, which is likely the case when domain size is not sufficiently larger than the correlation scale. The size of the domain for flow problem is required to be larger than that is required for solving the transport problem. Here to avoid the large computational cost, the domain is kept same for both flow and transport simulations. (L_x/l = 10.0 and L_y/l = 8.6).

[14] The computational efficiency and the accuracy of SFEM is presented in Table 2 in terms of mean and standard deviation of concentration at point P. The maximum error in $\overline{c}$ among the various test cases is found to be less than 3.5% while the error in standard deviation is found to be less than 8.0%. It is observed that in this case the errors in $\overline{c}$ and σ_c are increasing with correlation scale. Since the present method is first-order accurate for σ_c, in the case of 3-D problem, apart from the error in σ_c at a particular node, it may be required to compute the error in the steady state value of σ_c at several grid points of interest. One such scenario is to compute the error in σ_c at all the nodes in the domain. However, the concentration far way from the source for this problem is in general very low and the value is sensitive to the size of the domain and grid size. Hence one may consider only selected nodes where the mean concentrations are above a threshold level of interest. On the basis of this the error in σ_c can be defined as

$$\text{Error} = \frac{1}{N_c}\sum_{i=1}^{N_c}\frac{|\sigma_{c_i\text{SFEM}} - \sigma_{c_i\text{MCSM}}|}{\sigma_{c_i\text{MCSM}}} \tag{30}$$

where N_c is the number of nodes which are considered for error analysis. Four values of N_c are considered for calculation of the errors, which are as follows: (1) nodes in the computational domain, (2) nodes where $\overline{c} > 0.001$, (3) where $\overline{c} > 0.01$, and (iv) only one specific node at P as shown in Figure 4 is considered. Figure 7 shows the error in σ_c with respect to a range of values of coefficient of variation for two correlation scales. It is observed that the

Table 2. Values of Statistical Parameters and Comparison of Results for Different Cases in the 3-D Problem[a]

	COV							Error, %	
Case	n	k_d	γ_d	K	α	d_m	λ_h	$\overline{c}_{\text{iv}}$	$\sigma_{c\text{iv}}$
3A1	0.1	0.1	0.1	0.25	0.1	0.1	2.0	0.0	0.2
3A2	0.2	0.2	0.2	0.50	0.2	0.2	2.0	0.2	0.9
3A3	0.3	0.3	0.3	0.75	0.3	0.3	2.0	0.3	1.2
3A4	0.4	0.4	0.4	1.00	0.4	0.4	2.0	0.6	2.2
3A5	0.5	0.5	0.5	1.25	0.5	0.5	2.0	1.9	3.4
3B1	0.1	0.1	0.1	0.25	0.1	0.1	4.0	0.0	1.2
3B2	0.2	0.2	0.2	0.50	0.2	0.2	4.0	0.1	2.9
3B3	0.3	0.3	0.3	0.75	0.3	0.3	4.0	0.4	4.5
3B4	0.4	0.4	0.4	1.00	0.4	0.4	4.0	0.9	6.2
3B5	0.5	0.5	0.5	1.25	0.5	0.5	4.0	3.4	7.6

[a]CPU time is 175 s for SFEM and 334,200 s for MCSM.

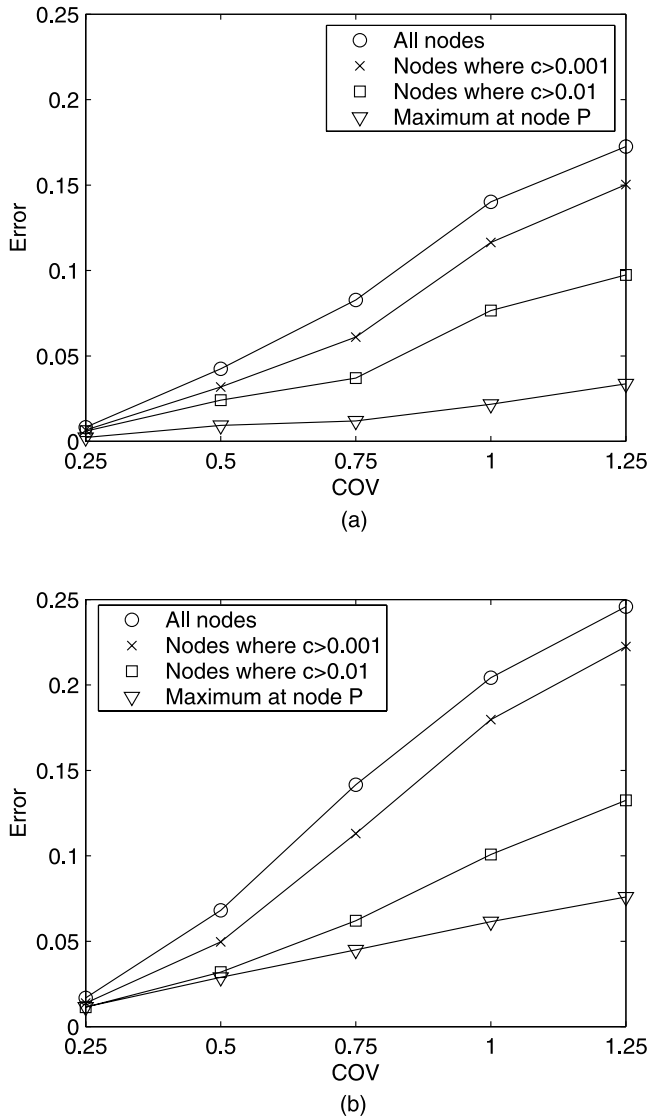

Figure 7. Errors in standard deviation of concentration in SFEM for different values of coefficient of variation (COV) of hydraulic conductivity and correlation scale (a) $\lambda_h = 2$ and (b) $\lambda_h = 4$ for the 3-D problem.

error in σ_c is the highest when all the nodes are considered while it is the least when error is computed at one point P (i.e., case iv). It is shown in Table 2 that computational time required for SFEM is approximately equal to 5 to 6 times that of the solution of the deterministic 3-D problem. This means the MCSM with 10000 realizations for this case is approximately 1800 times more computationally expensive. The higher efficiency (at least two orders) here is essentially due to the approach used in the SFEM for computing the derivatives of the concentration with respect to random parameters. It is interesting to note that the ratio of computational time is not much affected significantly between 1-D and 3-D problems, indicating the usefulness of this method for solving higher-dimension problems.

7. Conclusions

[15] Alternate approaches which are computationally efficient to MCSM and reasonably accurate are of interest for solution of stochastic partial differential equation in the case of flow and transport in heterogeneous porous medium. The present study proposes an efficient approach using SFEM, which is second-order accurate in mean and first-order accurate in the standard deviation. Comparison of SFEM is made with MCSM while estimating the mean and standard deviation of concentration for flow and transport in a porous medium with random hydraulic conductivity, porosity, dispersivity, molecular diffusion, sorption coefficient and first-order decay rate. Accuracy and computational efficiency of SFEM is compared with MCSM for one and three dimensional problems for various test cases with different coefficient of variation and correlation scale of the system parameters.

[16] The results with SFEM are obtained for moderate values of coefficient of variation (less than 125% for hydraulic conductivity and 50% for the rest of the random parameters) and are found to be good. The computational efficiency of SFEM is found to be significantly higher (several orders) than that of MCSM. The efficient performance of the present SFEM in comparison with standard SFEM is essentially due to use of derivatives of local matrices instead of global matrices while computing the derivatives of the concentration with respect to random parameters.

[17] The computational efficiency obtained using SFEM for one and three dimensional problems is nearly similar. For the range of correlation scale studied in the 3-D problem, it is found that the error associated with mean and standard deviation increases with correlation scale. It is noted that the coefficient of variation of concentration is higher for the 1-D problem than the 3-D problem for the examples selected here. This may be due to the higher level of mixing in the 3-D case due to the reduction in the effects of medium heterogeneity.

References

Bellin, A., S. Saladin, and A. Rinaldo (1992), Simulation of dispersion in heterogeneous porous formation: Statistics, first-order theories, convergence of computation, *Water Resour. Res.*, *28*, 2211–2227.

Brancik, L. (2000), An improvement of FFT-based numerical inversion of two-dimensional Laplace transforms by means of ϵ-algorithm. paper presented at ISCAS 2000: IEEE International Symposium on Circuits and Systems, Inst. of Electr. and Electron. Eng., Geneva, Switzerland, 28–31 May.

Chaudhuri, A., and M. Sekhar (2005), Analytical solutions for macrodispersion in a 3D heterogeneous porous medium with random hydraulic conductivity and dispersivity, *Transp. Porous Media*, *58*, 217–241.

Chin, D. A., and T. Wang (1992), An investigation of the validity of first-order stochastic dispersion theories in isotropic porous media, *Water Resour. Res.*, *28*(6), 1531–1542.

Cushman, J. H. (1997), *The Physics of Fluid in Hierarchical Porous Media: Angstroms to Miles*, Springer, New York.

Dagan, G. (1989), *Flow and Transport in Porous Formations*, Springer, New York.

Gelhar, L. W. (1993), *Stochastic Subsurface Hydrology*, Prentice-Hall, Upper Saddle River, N. J.

Ghanem, R. G., and P. D. Spanos (1991), *Stochastic Finite Elements: A Spectral Approach*, Springer, New York.

Haggerty, R., and S. M. Gorelick (1995), Multiple-rate mass transfer for modeling diffusion and surface reactions in media with pore-scale heterogeneity, *Water Resour. Res.*, *31*(10), 2383–2400.

Harleman, D. R. F., P. F. Mehlhorn, and R. R. Rumer (1963), Dispersion-permeability correlation in porous media, *J. Hydraul. Div. Proc. Am. Soc. Civ. Eng.*, *89*(2), 67–85.

Hassan, A. E. (2001), Water flow and solute mass flux in heterogeneous porous formations with spatially random porosity, *J. Hydrol.*, *242*, 1–25.

Hassan, A. E., J. H. Cushman, and J. W. Delleur (1999), A Monte Carlo assessment of Eulerian flow and transport perturbation models, *Water Resour. Res.*, *34*(5), 1143–1163.

Hu, B. X., J. H. Cushman, and F. W. Deng (1997), Nonlocal reactive transport with physical, chemical and biological heterogeneity, *Adv. Water Resour.*, *20*, 293–308.

Huang, H., and B. H. Hu (2000), Nonlocal nonreactive transport in heterogeneous porous media with interregional mass diffusion, *Water Resour. Res.*, *36*(7), 1665–1675.

Jang, Y. S., N. Sitar, and A. Der Kieoreghian (1994), Reliability analysis of contaminant transport in saturated porous media, *Water Resour. Res.*, *30*(8), 2435–2448.

Kapoor, V., and L. W. Gelhar (1994), Transport in three-dimensionally heterogeneous aquifers: 2. Prediction and observations of concentration fluctuations, *Water Resour. Res.*, *30*(6), 1789–1801.

Kleiber, M., and T. D. Hien (1992), *The Stochastic Finite Element Method*, John Wiley, Hoboken, N. J.

Li, S. G., F. Ruan, and D. McLaughlin (1992), A space-time accurate method for solving solute transport problem, *Water Resour. Res.*, *28*(9), 2297–2306.

Lu, Z., and D. Zhang (2004), A comparative study on uncertainty quantification for flow in randomly heterogeneous media using Monte Carlo simulations and conventional and KL-based moment-equation approaches, *SIAM J. Sci. Comput.*, *26*(2), 558–577.

Manohar, C. S., and R. A. Ibrahim (1999), Progress in structural dynamics with stochastic parameter variations 1987–1998, *Appl. Mech. Rev.*, *52*(5), 177–197.

Metzger, D., H. Kinzelbach, I. Neuweiler, and W. Kinzelbach (1999), Asymptotic transport parameters in a heterogeneous porous medium: Comparison of two ensemble-averaging procedures, *Stochastic Environ. Res. Risk Assess.*, *13*, 396–415.

Miralles-Wilhelm, F., and L. W. Gelhar (2000), Stochastic analysis of oxygen-limited biodegradation in heterogeneous aquifers with transient microbial dynamics, *J. Contam. Hydrol.*, *42*, 6997.

Osmani, S. (2002), Energy distributions estimation using stochastic finite element, *Renewable Energy*, *25*, 525–536.

Osnes, H. (1998), Stochastic analysis of velocity spatial variability in bounded rectangular heterogeneous aquifers, *Adv. Water Resour.*, *21*, 203–215.

Osnes, H., and H. P. Langtangen (1998), An efficient probabilistic finite element method for stochastic groundwater flow, *Adv. Water Resour.*, *22*(2), 185–195.

Ren, L., and R. Zhang (1999), Hybrid Laplace transform finite element method for solving the convection-dispersion problem, *Adv. Water Resour.*, *23*, 229–237.

Rowe, R. K., and J. R. Booker (1986), A finite layer technique for calculating three-dimensional pollutant migration in soil, *Geotechnique*, *36*(2), 205–214.

Schwarze, H., U. Jaekel, and H. Vereecken (2001), Estimation of macrodispersion by different approximation methods for flow and transport in randomly heterogeneous media, *Transp. Porous Media*, *43*, 265–287.

Spanos, P. D., and R. Ghanem (1989), Stochastic finite element expansion for random media, *J. Eng. Mech.*, *115*(5), 1035–1053.

Sudicky, E. A., and R. G. McLaren (1992), Laplace transform Galerkin technique for large-scale simulation of mass transport in discretely fractured porous formations, *Water Resour. Res.*, *28*(2), 499–514.

Tang, D. H., and G. F. Pinder (1979), Analysis of mass transport with uncertain physical parameters, *Water Resour. Res.*, *15*(5), 1147–1153.

Vanmarcke, E. H. (1983), *Random Field Analysis and Synthesis*, MIT Press, Cambridge, Mass.

Wu, J., B. X. Hu, and C. He (2004), A numerical methods of moments for solute transport in a porous medium with multiscale physical and chemical heterogeneity, *Water Resour. Res.*, *40*, W01508, doi:10.1029/2002WR001473.

Zhang, D. (1999), Nonstationary stochastic analysis of transient unsaturated flow in randomly heterogeneous media, *Water Resour. Res.*, *35*(4), 1127–1142.

Zhang, D. (2002), *Stochastic Methods for Flow in Porous Media: Coping With Uncertainty*, Elsevier, New York.

Zhang, D., and Z. Lu (2004), An efficient, higher-order perturbation approach for flow in random porous media via Karhunen-Loeve and polynomial expansions, *J. Comput. Phys.*, *194*, 773–794.

A. Chaudhuri and M. Sekhar, Department of Civil Engineering, Indian Institute of Science, Bangalore 560 012, India. (muddu@civil.iisc.ernet.in)